

Sergey V. Kalyuzhnyi · Vyacheslav V. Fedorovich
Piet Lens

Dispersed plug flow model for upflow anaerobic sludge bed reactors with focus on granular sludge dynamics

Received: 10 July 2004 / Accepted: 23 February 2005 / Published online: 8 April 2005
© Society for Industrial Microbiology 2005

Abstract A new approach to model upflow anaerobic sludge bed (UASB)-reactors, referred to as a one-dimensional dispersed plug flow model, was developed. This model focusses on the granular sludge dynamics along the reactor height, based on the balance between dispersion, sedimentation and convection using one-dimensional (with regard to reactor height) equations. A universal description of both the fluid hydrodynamics and granular sludge dynamics was elaborated by applying known physical laws and empirical relations derived from experimental observations. In addition, the developed model includes: (1) multiple-reaction stoichiometry, (2) microbial growth kinetics, (3) equilibrium chemistry in the liquid phase, (4) major solid-liquid-gas interactions, and (5) material balances for dissolved and solid components along the reactor height. The integrated model has been validated with a set of experimental data on the start-up, operation performance, sludge dynamics, and solute intermediate concentration profiles of a UASB reactor treating cheese whey [Yan et al. (1989) *Biol Wastes* 27:289–305; Yan et al. (1993) *Biotechnol Bioeng* 41:700–706]. A sensitivity analysis of the model, performed with regard to the seed sludge characteristics and the key model parameters, showed that the output of the dispersed plug flow model was most influenced by the sludge settleability characteristics and the growth properties (especially μ_m) of both protein-degrading bacteria and acetotrophic methanogens.

Keywords Mathematical model · Upflow anaerobic sludge bed reactor · Dispersion · Plug flow · Sedimentation

Nomenclature

<i>A</i>	Coefficients in empirical equations
AC	Ash content of the dry sludge aggregates (%)
<i>b</i>	Bacterial (death + lysis) rate coefficient (day^{-1})
COD	Chemical oxygen demand (g)
CS	Reactor cross section (dm^2)
<i>d</i>	Aggregate diameter (dm)
<i>D</i>	Dispersion coefficient ($\text{dm}^2 \text{day}^{-1}$)
<i>g</i>	Gravitational acceleration ($\text{dm} \text{day}^{-2}$)
<i>H</i>	Height of reactor liquid phase
He	Henry coefficient [$\text{atm} \text{dm}^3 \text{g}^{-1} \text{COD}(\text{mol})$]
HRT	Hydraulic retention time (days)
k_{La}	Mass transfer coefficient (day^{-1})
K_S	Monod half velocity constant (g COD dm^{-3})
<i>M</i>	Mass transfer rate to the gas phase [$\text{g COD}(\text{mol}) \text{dm}^{-3} \text{day}^{-1}$]
MC	Moisture content (%)
<i>n</i>	Number of sludge aggregates in the reactor
<i>N</i>	Component
OLR	Organic loading rate ($\text{g COD dm}^{-3} \text{day}^{-1}$)
<i>p</i>	Pressure (atm)
pK	pH drop-off value (at which growth rate = 50% of inhibited rate)
<i>q</i>	Surface gas production rate ($\text{dm}^3 \text{dm}^{-2} \text{day}^{-1}$)
<i>Q</i>	Gas volumetric flow rate from the reactor ($\text{dm}^3 \text{day}^{-1}$)
<i>r</i>	Biotransformation rate (g COD dm^{-3})
<i>S</i>	Substrate concentration in liquid phase [$\text{g COD}(\text{mol}) \text{dm}^{-3}$]
SLR	Sludge loading rate ($\text{g COD g}^{-1} \text{VSS day}$)
SRT	Sludge retention time (days)
<i>t</i>	Time (days)
<i>T</i>	Temperature (K)
TKN	Total Kjeldahl nitrogen (g)
TP	Total phosphorus (g)
TS	Total solids (g)
TSS	Total suspended solids (g)

S. V. Kalyuzhnyi (✉) · V. V. Fedorovich
Department of Chemical Enzymology,
Chemistry Faculty,
Moscow State University,
119899, Moscow, Russia
E-mail: svk@enz.chem.msu.ru
Tel.: +7-95-9395083
Fax: +7-95-9395417

P. Lens
Sub-department of Environmental Technology,
Wageningen University,
PO Box 8129,
6700 EV Wageningen,
The Netherlands

UASB	Upflow anaerobic sludge bed
V_{ag}	Volume of one spherical aggregate
V_G	Volume of reactor gas phase (dm^3)
V_m	Specific molar volume of gas under given temperature [$\text{dm}^3 \text{g}^{-1} \text{COD}(\text{mol})$]
V_R	Volume of reactor liquid phase (dm^3)
VFA	Volatile fatty acids
VS	Volatile solids (g)
VSS	Volatile suspended solids (g)
W	Terminal vertical velocity (dm day^{-1})
W_s	Settling velocity (dm day^{-1})
W_{up}	Upward liquid velocity (dm day^{-1})
X	Biomass concentration (g l^{-1})
Y	Bacterial yield ($\text{g VSS g}^{-1} \text{COD consumed}$)
z	Distance from the reactor input (dm)

Greek symbols

ϵ	Solid hold up (dimensionless)
η	Viscosity ($\text{g dm}^{-1} \text{day}^{-1}$)
μ	Specific growth rate (day^{-1})
μ_m	Maximum specific growth rate (day^{-1})
ρ	Density (g dm^{-3})
ψ	Parameters in the solids dynamics expressions

Subscripts and superscripts

0	Influent
*	Undissociated form
ag	aggregate
G	Gas
I	Substrate I
j	Bacteria j
L	Liquid
sl	Sludge
tot	Total

Introduction

The upflow anaerobic sludge bed (UASB) reactor [20] is currently the most popular reactor design for high rate anaerobic treatment of industrial wastewater [19]. The success of this reactor concept is based mainly on the ability of anaerobic bacteria to form dense aggregates by autoimmobilisation. As these aggregates have much higher settling velocities ($20\text{--}80 \text{ m h}^{-1}$) than the applied upflow velocities ($W_{up}=0.1\text{--}1 \text{ m h}^{-1}$), high biomass concentrations can accumulate in the reactor. Thus, high sludge loading rates (SLR up to $5 \text{ g COD g}^{-1} \text{ VSS}^{-1} \text{ day}^{-1}$) can be applied at relatively short hydraulic retention times (HRT less than 4 h).

With respect to the concentration of the aggregates along the reactor height, three zones are usually distinguished inside a UASB reactor: (1) a dense sludge bed consisting of biomass aggregates in the bottom section, (2) a sludge blanket containing finely suspended flocs or aggregates, and (3) a zone of clarified water containing almost no solids in the internal settler. This heterogeneous sludge distribution along the height of the UASB reactor excludes the application of the majority of the numerous mathematical models developed for completely mixed anaerobic digestion systems, as these models assume a homogeneous biomass distribution and hydrodynamic pattern within the reactor.

In some models, the heterogeneous hydrodynamic pattern of a UASB reactor has been described by dividing its total volume into two or more compartments. Each of these compartments is assumed to have ideal attributes (such as ideal mixing or plug flow), and they are linked with each other by bypassing and back mixing flows [3, 10, 11, 36]. These multi-compartment models are generally capable of fitting experimental data quite satisfactorily for UASB reactors operating under steady-state conditions. However, the calibration of these models relies on detailed experimental tracer studies to determine the volume fraction of each compartment and the degree of bypass flow for each regime modelled. Moreover, many of these tracer studies deal only with short-term impulse loadings of a soluble tracer under steady-state conditions and thus neglect the dynamics of solid components (e.g. granules migrating between different compartments). Unsteady state conditions (e.g. during start-up of the UASB reactor or overloading) as well as granular sludge dynamics inside the reactor are the most critical points of multi-compartment models, which hamper their application for real-time control strategies.

A continuous description of solids dynamics along the reactor height has been developed for three-phase fluidised bed systems [7, 13, 39]. Although there are clear differences between UASB ($W_{up}=0.1\text{--}1 \text{ m h}^{-1}$, no carrier) and fluidised bed reactors (W_{up} up to 20 m h^{-1} , sandy material as carrier), these approaches can also be used to describe the multiple solid-liquid-gas interactions that take place in UASB reactors. In biochemical and environmental engineering, modelling efforts for biological fluidised-bed reactors have been directed mainly towards description of reactor hydrodynamics [4, 8, 35], whereas description of sludge dynamics has hardly been addressed. In chemical engineering, however, mathematical models that describe accurately the solids dynamics in fluidised bed reactors have been developed [28, 34]. A straightforward application of the solids dynamics ideology proposed for chemical fluidised-bed reactors to the modelling of UASB reactors is practically impossible because of the extreme complexity of the mathematical methods used (e.g. numerous non-linear equations with partial derivatives) and the different time scale of the physical (very quick) and biological (relatively

slow) processes in UASB reactors. Despite these limitations, adoption of some ideas from solid dynamics in chemical three-phase fluidised bed reactors can contribute significantly to a more accurate modelling of the performance of UASB reactors.

The objective of the present work was to develop an integrated mathematical model for the UASB reactor concept, combining granular sludge dynamics, solid-liquid-gas interactions and hydrodynamics, with biological conversions (multiple reaction stoichiometry, microbial growth kinetics) and liquid phase equilibrium chemistry. The integrated model was subsequently validated with existing experimental data on the start-up and operational performance of UASB reactors. Finally, a sensitivity analysis of the key model parameters was performed.

Model postulates and development for granular sludge dynamics and hydrodynamics

In the present model, all processes (physical, chemical and microbiological) inside the reactor are considered to depend only on the vertical axis of the reactor (distance z from input, z varies from 0 to H) and time t . Thus, all the process characteristics in a fixed reactor cross-section CS_z are assumed to be uniform. In general, the space distribution of the concentration of any component N (soluble or suspended) along the reactor height z can be expressed on the basis of the dispersed plug flow concept [21] using the following equation:

$$\frac{\partial}{\partial t} N(z, t) = \frac{\partial}{\partial z} \left[D(z, t) \cdot \frac{\partial}{\partial z} N(z, t) \right] - \frac{\partial}{\partial z} [W(z, t) \cdot N(z, t)] + r(z, t) - M(z, t) \quad (1)$$

The first term in the right part of Eq. 1 characterises the degree of mixing by gas-induced dispersion. The second term determines a convective transport of component N in the vertical direction. The third and fourth terms are the net biotransformation rate and transfer rate to the gas phase for component N , respectively. The boundary conditions for Eq. 1 follow from the relationship between the internal mass transfer given by Fick's first law and external mass transfer given by Newton's law [see 23]:

$$D(0, t) \cdot \frac{\partial}{\partial z} N(0, t) = W(0, t) \cdot [N(0, t) - N^0] \quad (2)$$

$$D(H, t) \cdot \frac{\partial}{\partial z} N(H, t) = 0 \quad (3)$$

The specification of Eq. 1 for solid, soluble and gaseous components of the UASB reactor as well as the assumptions introduced to enable the numerical solution of Eq. 1 are considered below.

Solid components

In the case of wastewaters containing only soluble substrates, the solids in the reactor consist only of sludge aggregates (granules or flocs) containing active biomass of different bacterial groups and biologically inactive VSS. The main bottleneck in the application of Eq. 1 for granular sludge is the derivation of a mathematical expression for the vertical velocity $W(z, t)$ and the dispersion coefficient $D(z, t)$ of the sludge aggregates.

Vertical velocity of granular sludge

In general, the value of $W(z, t)$ for any component N is determined by the balance between the upward velocity $W_{\text{up}}(z, t)$ and the apparent settling velocity $W_s(z, t)$:

$$W(z, t) = W_{\text{up}}(z, t) - W_s(z, t) \quad (4)$$

Under negligible solid hold-up, the upward velocity can be approximated to:

$$W_{\text{up}} = \frac{V_R}{\text{HRT} \cdot CS} \quad (5)$$

The expression for $W_s(z, t)$ for sludge solids can be derived from the Stokes law under $\text{Re} < 2$, the region in which UASB reactors usually operate [33]:

$$W_s(z, t) = \frac{[\Psi_1 \cdot \rho_{\text{ag}}(t) - \rho_L] \cdot g \cdot d_{\text{ag}}^2(t)}{18 \cdot \eta(z, t)} \quad (6)$$

where Ψ_1 represents the influence of gas entrapment and attachment on the apparent aggregate density. It should be noted that $W_s(z, t)$ in Eq. 6 represents the average velocity of the sludge solids in a cross-section CS_z along the z -axis. Thus, $W_s(z, t)$ is clearly different from the usually measured instantaneous settling velocity of unfed and degassed aggregates [1]. There are some problems in calculating the settling velocity for suspensions with high solid concentrations, e.g. granular sludge suspensions in UASB reactors, because they behave as non-Newtonian liquids. These suspensions are often referred to as pseudo-Newtonian liquids and several empirical formulas to calculate their viscosity are available in engineering practice [7]. The formula used in our model is directly taken from Darton's review [7]:

$$\eta(z, t) = \eta_L \exp[A_1 \varepsilon(z, t)^{2.5}] \quad (7)$$

The solid hold up $\varepsilon(z, t)$ given in Eq. 7 can be calculated from its physical definition:

$$\varepsilon(z, t) = \frac{\text{VSS}_{\text{tot}}(z, t)}{\left(1 - \frac{\text{AC}_{\text{ag}}}{100}\right) \cdot \left(1 - \frac{\text{MC}_{\text{ag}}}{100}\right) \cdot \rho_{\text{ag}}(t)} \quad (8)$$

Besides the liquid viscosity, the expression for $W_s(z, t)$ in Eq. 6 also includes the time dependency of the aggregates density $\rho_{\text{ag}}(t)$ and their average diameter $d_{\text{ag}}(t)$. Since the granule density usually does not vary

significantly during an experimental run with a single type of wastewater [1, 12, 27], the aggregate density is assumed to be constant in the current version of the model. Additionally, aggregates were assumed to have a spherical form and the same (but variable with time) diameter within the entire reactor (see below). These simplifying assumptions were introduced to make the model workable, although they do not completely reflect reality. Extension of these assumptions to more realistic conditions (e.g. introduction of the size distribution of the sludge, variable density with time) will be the next step in the development of this modelling concept.

The average granule diameter was found to have a positive relationship with the sludge loading rate [1, 24] and the influent concentration [9]. Both parameters are often related, and determine substrate penetration depth and thus, indirectly, aggregate size. Since it is rather problematic to formalise the observed dependencies between the average aggregate diameter and the factors mentioned above, a more simple relation dealing with the net sludge growth/decay [5] was used in the model:

$$\begin{aligned} \frac{d[d_{ag}(t)]}{dt} &= \frac{2}{\pi \cdot d_{ag}^2(t)} \cdot \frac{dV_{ag}}{dt} \\ &= \frac{\psi_2}{n(t)} \cdot \frac{2}{\pi \cdot d_{ag}^2(t)} \\ &\quad \cdot \frac{\int_0^H \left[\sum_j (\mu_j(z, t) - b_j) \cdot X_j(z, t) \right] \cdot CS \cdot dz}{\left(1 - \frac{AC_{ag}}{100}\right) \cdot \left(1 - \frac{MC_{ag}}{100}\right) \cdot \rho_{ag}(t)} \end{aligned} \quad (9)$$

This equation is derived from the evident link between the diameter and the volume of a spherical sludge aggregate. The function $n(t)$ is the number of aggregates in the reactor, whereas the parameter ψ_2 aims to account for additional changes in the average granule diameter due to aggregation/disaggregation processes. The number of aggregates in the reactor can be expressed by dividing the total sludge volume (V_{sl}) by the ‘‘average’’ volume of one aggregate (V_{ag}):

$$n(t) = \frac{V_{sl}}{V_{ag}} = \frac{VSS_R(t)}{\left(1 - \frac{AC_{ag}}{100}\right) \cdot \left(1 - \frac{MC_{ag}}{100}\right) \cdot \rho_{ag}(t)} \cdot \frac{6}{\pi \cdot d_{ag}^3(t)} \quad (10)$$

Substituting Eq. 10 into Eq. 9, one obtains:

$$\begin{aligned} \frac{d[d_{ag}(t)]}{dt} &= \psi_2 \cdot \frac{d_{ag}}{3} \\ &\quad \cdot \frac{\int_0^H \left[\sum_j (\mu_j(z, t) - b_j) \cdot X_j(z, t) \right] \cdot CS \cdot dz}{VSS_R(t)} \end{aligned} \quad (11)$$

Although Eq. 11 is an oversimplification of the real situation, it is a reasonable empirical relation, which overcomes the lack of more mechanistic expressions.

Dispersion of granular sludge

A formulation for $D(z, t)$ in the blanket zone of UASB reactors was proposed by Narnoli and Mehrotra [26] on the basis of the so-called diffusion concept:

$$D(z, t) = A_2 \cdot \left[q(z, t) \cdot \left(1 - \exp\left(-\frac{A_3}{q(z, t)}\right) \right) \right]^2 \quad (12)$$

This expression has been found to be valid on the basis of experimental observations available in the literature on solids concentrations in the sludge blanket zone of UASB reactors. It should be noted that Eq. 12 is similar to several expressions proposed earlier for the calculation of the dispersion coefficients in three-phase fluidised beds reactors [7]. In all these formulations, the value of $D(z, t)$ is highly dependent on the surface gas production $q(z, t)$. In our model, Eq. 12 was used to describe the dispersion of solids throughout the reactor height.

Soluble components

For fluidised bed systems, the formula for the calculation of the dispersion coefficients $D(z, t)$ of solutes was shown not to differ principally from the dispersion coefficients of the suspended solids [7] due to the physical link between solids and liquid dispersion. Therefore, Eq. 12 was used in the model for the description of solute dispersion coefficients throughout the reactor height. Due to the negligible settling velocity of solutes, the upward velocity W_{up} (Eq. 5) exclusively determines their vertical velocity.

Gaseous components

Although anaerobic reactors have a gas hold up, it is usually relatively low, e.g. varying between 0.01 and 0.05 of the reactor volume depending on the surface gas production [4]. To avoid excessive intricacy, the gas hold up is neglected in the current version of the model, except for its influence on the apparent density of sludge aggregates (parameter ψ_1 , see Eq. 6). The gaseous components (methane, hydrogen, carbon dioxide and ammonia) are treated in the model as solutes, taking into account their transfer to the gas phase, which is considered as an ideally mixed medium. Studies on bubble columns have shown that the mass transfer coefficient k_{La} depends mainly on the surface gas production $q(z, t)$, and various formulations have been proposed [7, 39] for the description of this dependency. The following formula was used in the present model to describe the mass-transfer coefficients of components from the liquid to gas phase [39]:

$$k_{La}(z, t) = A_4 \cdot \left[\frac{q(z, t)}{A_5} \right]^{A_6} \quad (13)$$

Integration of biological and chemical building blocks into the model

Biotransformation kinetics

The present model simulates the anaerobic treatment of soluble organic wastewater, which can be represented by a three-step process: acidogenesis, acetogenesis, and methanogenesis. Each of these steps is carried out by separate groups of bacteria. The kinetic description of biotransformations was adapted from our previous models [14–17] and is based on the following assumptions:

- Each reaction rate is catalysed by the corresponding bacterial group j . Their growth proceeds according to Monod kinetics with pH modulation:

$$\mu_j = \mu_{m,j} \times \frac{S_i}{K_{S_j} + S_i} \cdot F(\text{pH}) \quad (14)$$

$$F(\text{pH}) = \frac{1 + 2 \times 10^{-(\text{pK}_{1,j} - \text{pK}_{2,j}) \cdot 0.5}}{10^{\text{pK}_{2,j} - \text{pH}} - 10^{\text{pH} - \text{pK}_{1,j}}} \quad (15)$$

- All product formations are directly coupled to bacterial growth. Substrate consumption for maintenance is incorporated in the overall biomass yield.
- The processes of bacterial death and cell lysis are combined and described by first order kinetics via the parameter b .
- Though diffusion limitation in biomass, aggregates can vary through the run (because aggregates have a variable average diameter over time), this effect was assumed constant in time in the present version of the model and was incorporated into the kinetic term via the apparent K_s . Although this assumption simplifies reality, its application is justified to some extent by the sensitivity analysis, which showed that the sensitivity of the model to this group of parameters is lower in comparison with other parameters (see below).

Equilibrium chemistry

Since the pH influences microbial kinetics (Eq. 14), the pH values in any compartment of the reactor liquid phase were calculated from the equation of electroneutrality, which included all the ionised species in this compartment. The approach used was described previously [14].

Material balances

Material balances for all the components involved are generalised in Appendix 1 for gas and liquid phases.

Dispersed plug flow model for UASB reactors

Model equations

The developed sets of equations (Eqs. 1, 2, 3, 4, 5, 6, 7, 8, 9, 10, 11, 12, 13, 14, 15, and 17, 18, 19, 20, 21, 22, 23, 24, 25, 26, 27, 28, 29) represent a general form of an integrated structured model of a UASB reactor. This is, to the best of our knowledge, the first model to combine solid-liquid-gas interactions, hydrodynamics, liquid phase equilibrium chemistry, and detailed microbiological substrate conversion. Since the internal reactor dynamics of the components involved are represented by balances between convection (Eq. 5), sedimentation (Eq. 6) and dispersion (Eq. 12), the model is called the dispersed plug flow model for UASB reactors.

Computational methods

Model simulations were performed on an IBM-compatible personal computer (processor Pentium-200) using a program written in Fortran-90. The program was generalised in such a way that a variable number of conversion reactions, organisms, components, and substrates, as well as data on the seed sludge, could be specified through an input file. The program created an output data file in a format suitable for graphic processing in Microsoft Excel.

The overall program contains three main routines for numerical solution of (1) high degree algebraic equations by iteration technique [18] for calculation of pH and concentrations of dissociated species, (2) the system of first-order differential equations by Runge-Kutta (fourth order) technique [23] for the calculation of the partial pressures of gases (Eq. 17), and (3) the system of second-order differential equations with two point boundary conditions (Eqs. 21, 22, 23, 24, 25, 26, 27) for calculation of the reactor height distribution of the component involved. The first two routines were taken from a previous program [16] with minor modifications. The third included discretisation of the first- and second-order derivatives of the system of second-order differential equations, followed by resolution of the algebraic system obtained with the iteration technique described by Samarskiy [32].

Model validation

Brief description of case study

Results from an experimental study by Yan et al. [37, 38] on the treatment of high strength cheese whey in a UASB reactor were used to validate the integrated structured model developed above. Salient features of the experimental protocol used are given in Table 1. Briefly, the UASB reactor was fed by cheese whey

Table 1 Details of the experimental study used in validation of the model [37, 38]

Parameter (dimension)	
Reactor design	
Working reactor volume (dm ³)	14.5
Inner diameter (dm)	1.15
Height of liquid phase (dm)	13.8
Wastewater characteristics	
Cheese whey composition (g dm ⁻³)	TS 56.6–58.9, VS 45.2–47, COD 64–67, TKN 2.75–3.05, NH ₄ ⁺ -N 0.0028–0.00295, NO ₃ ⁻ -N 0.00045–0.0007, TP 0.338–0.356, VFA 0.066–0.45, pH 4–6
Influent COD (g dm ⁻³)	4.6–38.1
Mineral medium content (g 14 dm ⁻³)	NaHCO ₃ (2.0), K ₂ HPO ₄ (6.6), NH ₄ Cl (1.0), Fe ³⁺ (0.04), Mg ²⁺ (0.01)
Influent pH	Adjusted to pH 7.0 with NaOH
Operational characteristics	
Temperature (°C)	33 ± 1
HRT (days)	5
OLR (g COD dm ⁻³ day ⁻¹)	0.91–7.77
Seed sludge	4 L (3% TS, 2.1% VS) ^a

^a67.2 g VSS of the same sludge was added at day 15

diluted in different proportions with a mineral medium under a constant HRT of 5 days. Start-up and steady-state performance of the reactor under an OLR increase from 0.91 to 7.62 g COD dm⁻³ day⁻¹ were investigated in detail. The corresponding concentration profiles (COD, VFA, pH) along the reactor height were thoroughly documented. The time schedule of the experimental runs used for the model validation is presented in Table 2. The specification of our model to this case study is presented in Appendix 2.

Selection of model parameters and seed sludge characteristics

The physico-chemical model parameters, e.g. dissociation constants and Henry constants, were directly transferred from a previous model [16]. Bacterial parameters (Table 3) were also adapted from previous models [14, 16] after minor correction tuning. The majority of the parameters determining solids dynamics were directly taken from the literature (Table 4). The remaining parameters in Table 4 were tuned to fit the data of Yan et al. [37, 38] using literature analogies (where possible) as first approximations. The rationale behind these choices is described briefly below.

Since the ash content is a main factor determining granule density [12], the latter was fixed at 1,026 g dm⁻³ in the model (Table 4), based on analogy with granules with a similar ash content reported by Alphenaar [1]. The diameter of granular sludge aggregates varies

between 0.14 and 5 mm [33]. Taking into account that the seed used had poor settleability [37], the initial average diameter of the sludge aggregates was taken to be close to the lower boundary of the above mentioned interval (Table 4). A rough estimation of a value for ψ_1 can be made using the typical gas hold-up of anaerobic reactors, namely, 0.01–0.05 [4]. This means that ψ_1 can vary between 0.95 and 0.99. More fine-tuning leads to the value listed in Table 4.

Since the seed sludge characteristics were not given in Yan et al. [37, 38], the initial quantity of the various bacterial groups involved, as well as inactive VSS, in the seed sludge (total quantity of VSS inoculated to the reactor was 86.54 g) was arbitrarily fixed in the model as follows (g VSS per reactor):

$$\begin{aligned} X_1 &= 0.57; X_2 = 0.92; X_3 = 4.74; X_4 = 8.44; X_5 \\ &= 0.57; \text{VSS}_{\text{inact.}} = 71.3 \end{aligned} \quad (16)$$

To assess the effect of these assumptions on the final result of the fit, a sensitivity analysis of the model to its parameters and the seed sludge characteristics was performed (see below).

Calculation accuracy

The primary problem that arises under numerical integration of such a complex non-linear system like the set of equations developed here (Eqs. 1, 2, 3, 4, 5, 6, 7, 8, 9, 10, 11, 12, 13, 14, 15, 17, 18, 19, 20, 21, 22, 23, 24, 25, 26,

Table 2 Time schedule of the experimental runs [37, 38] used in the validation of the dispersed plug flow model

Running period	OLR (g COD dm ⁻³ day ⁻¹)	Influent COD (g COD dm ⁻³)	Run time (days)
I (0–30 days)	0.91	4.6	30
II (31–58 days)	1.97	9.9	28
III (59–94 days)	3.54	17.7	36
IV (95–125 days)	5.96	28.8	31
V (126–143 days)	7.62	38.1	18

Table 3 Kinetic parameters of the different bacterial groups used in the simulations

Bacterial group	μ_m (day ⁻¹)	K_S (gCOD dm ⁻³)	Y (gVSS g ⁻¹ COD)	b (day ⁻¹)	$p K_1$	$p K_2$
X ₁	0.80	0.30	0.050	0.15	4.0	7.25
X ₂	0.21	0.70	0.022	0.05	4.35	6.9
X ₃	0.17	0.31	0.020	0.02	5.65	7.5
X ₄	0.22	0.30	0.021	0.02	5.65	7.5
X ₅	0.42	0.00048	0.011	0.12	5.65	7.5
Inactive VSS	–	–	–	0.02	–	–

27, 28, 29) is the accuracy of the algorithm applied. Since, at each step of numerical integration, at least minor errors in calculation are always generated due to the use of discretisation and linearisation procedures, the resulting cumulative error can be big enough to produce significant deviations in, for example, the mass balance of the modelled system. The usual way to minimise such problems is to select small integration steps for the variables z and t . However, integration steps that are too small lead to an enormous increase in computer calculation time, which impedes, or can even preclude, model validation. After some preliminary simulation trials, a reasonable compromise between accuracy and calculation time was found for $\Delta t = 0.000125$ days and $\Delta z = H/100 = 0.138$ dm. Under these conditions, the calculation time of a complete reactor run (143 days) was around 15 h and the deviations of the daily COD balance never exceeded 8% (Fig. 1a). It should be noted that such deviations were less than, or around, 2% throughout almost the complete reactor run, and were higher only in periods IV–V when the values of the dispersion coefficient and settling velocity became high (Fig. 1b, c).

Analysis of model predictions vs the experimental case study

The results of superimposing experimental data and model predictions are presented in Figs. 2, 3, 4, 5 and 6. In general, the predictions agree satisfactorily with the

experimentally recorded data during the start-up period (Fig. 2) as well as with the reported steady-state performance indicators (Fig. 3) and sludge characteristics (Fig. 4) under the various OLR applied.

The model slightly overestimates the effluent VSS during the start-up period (Fig. 2b) and a cumulative VSS washout during the periods I–IV (Fig. 4b). However, a satisfactory agreement between the simulations and the experimental observations was obtained for the total quantity of VSS in the reactor (Fig. 4a) and the SLR at the end of each operational period (Fig. 4c). On the other hand, the model underestimates the steady-state effluent COD during periods III–V (Fig. 3a) and, as a result, overestimates the methane production in the same periods (Fig. 3b). These discrepancies can be attributed mainly to the simplified description of the VSS dynamics and, consequently, inaccurate description of bacterial transport along the reactor height in the dispersed plug flow model. As stated above, aggregate transport is governed by dependencies more complex than those postulated in the model (Eqs. 6, 11, 12). The dynamics of the factors influencing VSS behaviour in the model are presented in Fig. 1b,c. It can be seen that the calculated average sludge diameter gradually increased throughout the experimental run, resulting in a substantial increase in the settling velocity (Fig. 1b), which agrees with the experimental observations of Yan et al. [37]. It should also be noted that the dispersion coefficient reacts more sharply than the settling velocity upon an increase in OLR (Fig. 1b,c). This is because the value of the dispersion coefficient D is indirectly very sensitive

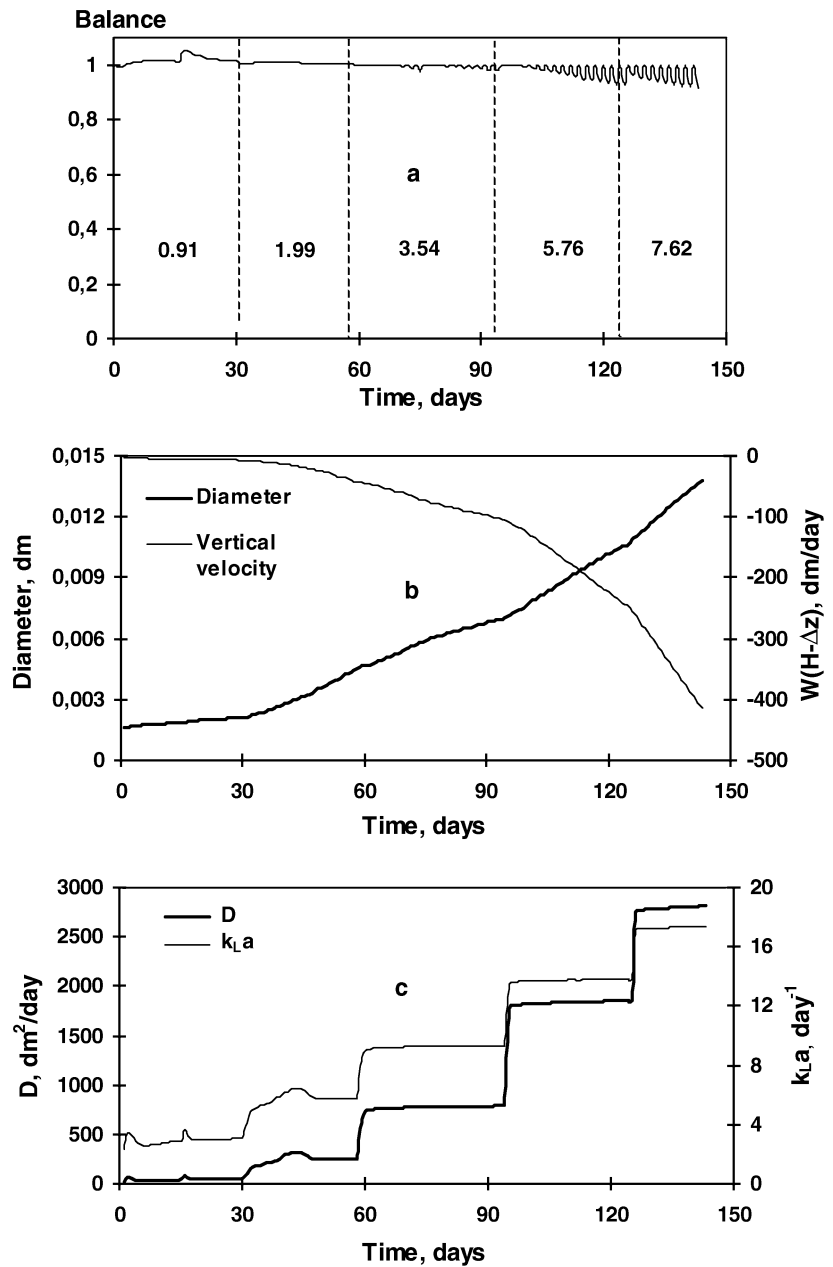
Table 4 Parameters determining solids dynamics used in the simulations

Parameter (dimension)	Value	Reference
A ₁ (dimensionless)	36.5	Darton [7]
A ₂ (day ⁻¹)	0.83 ^a	Narnoli and Mehrotra [26]
A ₃ (dm day ⁻¹)	132 ^a	Narnoli and Mehrotra [26]
A ₄ (day ⁻¹)	40,348.8 ^a	Zhukova [39]
A ₅ (day dm ⁻¹)	864,000	Transfer coefficient for $q(z, t)$ from ms ⁻¹ into dm day ⁻¹
A ₆ (dimensionless)	0.82	Zhukova [39]
η_L (g dm ⁻¹ day ⁻¹)	6.921 ^b	Rabinovich and Khavin [30]
ρ_L (g dm ⁻³)	997 ^b	Rabinovich and Khavin [30]
AC _{ag} (%)	30	Yan et al. [37]
MC _{ag} (%)	87.5	Bailey and Ollis [2]
ρ_{ag} (g dm ⁻³)	1.026	Extrapolation from Alphenaar [1]
d_0 (dm)	0.00155	Extrapolation from Schmidt and Ahring [33]
ψ_1 (dimensionless)	0.9721	This study (fitted)
ψ_2 (dimensionless)	22,500	This study (fitted)

^aRecalculated from original data

^b30°C

Fig. 1 Model simulation of the evolution as a function of time of **a** daily COD balance of the system, **b** sludge average diameter and vertical velocity, and **c** dispersion and mass transfer coefficient in the settler zone of the reactor. Figures on the plot area in **a** represent the OLR applied ($\text{g COD dm}^{-3} \text{ day}^{-1}$)



to the OLR via the surface gas production q (Eq. 20). Finally, the model predicts the pH values in the effluent fairly well (Fig. 3c). Minor discrepancies during the first two periods could be due to the presence of some ionised components in the raw cheese whey, which are not considered in the model stoichiometry (Appendix 2).

A satisfactory agreement between model and experiment was also obtained for the COD- and pH-profile along the reactor height (Figs. 5, 6). The major discrepancies were found at an OLR of $7.62 \text{ g COD dm}^{-3} \text{ day}^{-1}$ for both pH- and COD-profiles (Figs. 5d, 6e), namely, a prolonged plug-flow region was experimentally observed in the bottom of the sludge bed whereas the model predicts this region as more narrow. The reason might be related to the inadequate description of dispersion at the reactor bottom, i.e. the model

overestimates surface gas production during period V, which determines the value of the dispersion coefficient (Eq. 12). Changing the stoichiometric coefficients in Eqs. 30 and 31 towards decreasing gas production was an inappropriate measure to obtain a better fit of the data, because it led to reactor failure (acidification) during period II (data not shown). It should also be noted that the reaction products formed during acidogenesis are very flexible, i.e. different products can be formed from the same substrate by different microorganisms. Moreover, even the same organism can form different products depending on the pH [40]. This flexibility in intermediates of the acidogenic step was not taken into account in the model and could be another reason for the observed discrepancy in the pH- and COD-profiles during period V.

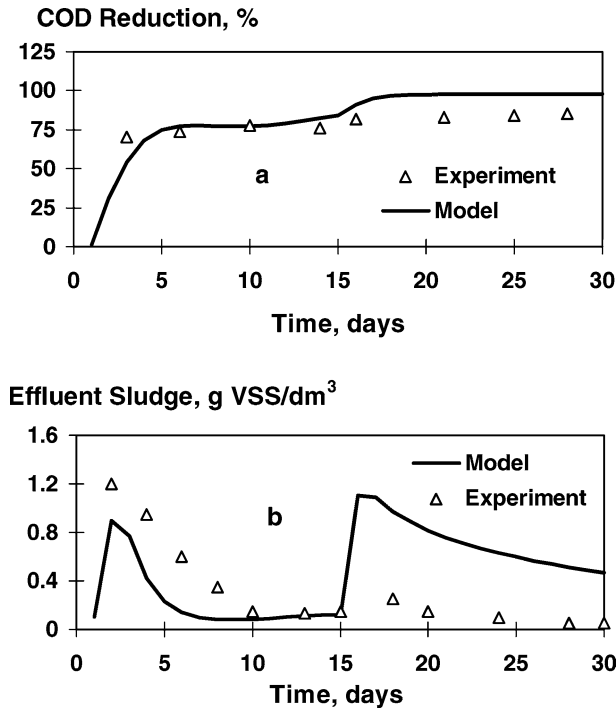


Fig. 2 Model vs experiment during start-up period for **a** total COD removal and **b** effluent VSS. Experimental data taken from Yan et al. [37]

Sensitivity analysis

Considering the large number of variable model parameters (33 in total) and the rather arbitrary fixation of the seed sludge characteristics (5 in total), one might expect significant difficulties in parameter identification. Thus, it was of primary importance to investigate the sensitivity of the model to these parameters.

The results of the sensitivity analysis for the seed sludge characteristics are shown in Fig. 7. With respect to the microbiological characteristics (Fig. 7a), the model is most sensitive to the initial concentrations of the bacterial groups X_2 and X_4 . Moreover, a decrease of 20% in the initial concentration of X_4 in the seed leads to reactor acidification during period II (data not shown). These results can be interpreted on the basis that both protein-degrading bacteria X_2 (via formation of VFA and ammonia) and acetotrophic methanogens X_4 (via consumption of acetate) play a key role in the formation of the reactor pH. The low sensitivity of the model to the initial concentration of propionate-degrading bacteria X_3 was at first surprising, as propionate accumulation has been often associated with reactor failure [6]. It becomes understandable when one takes into account the low impact of the corresponding conversion reaction (Eq. 32) to the generation of acidity in the system. The very low sensitivity of the model to the initial concentration of the lactose-degrading bacteria X_1 and hydrogenotrophic methanogens X_5 is quite obvious because both bacteria are relatively fast grow-

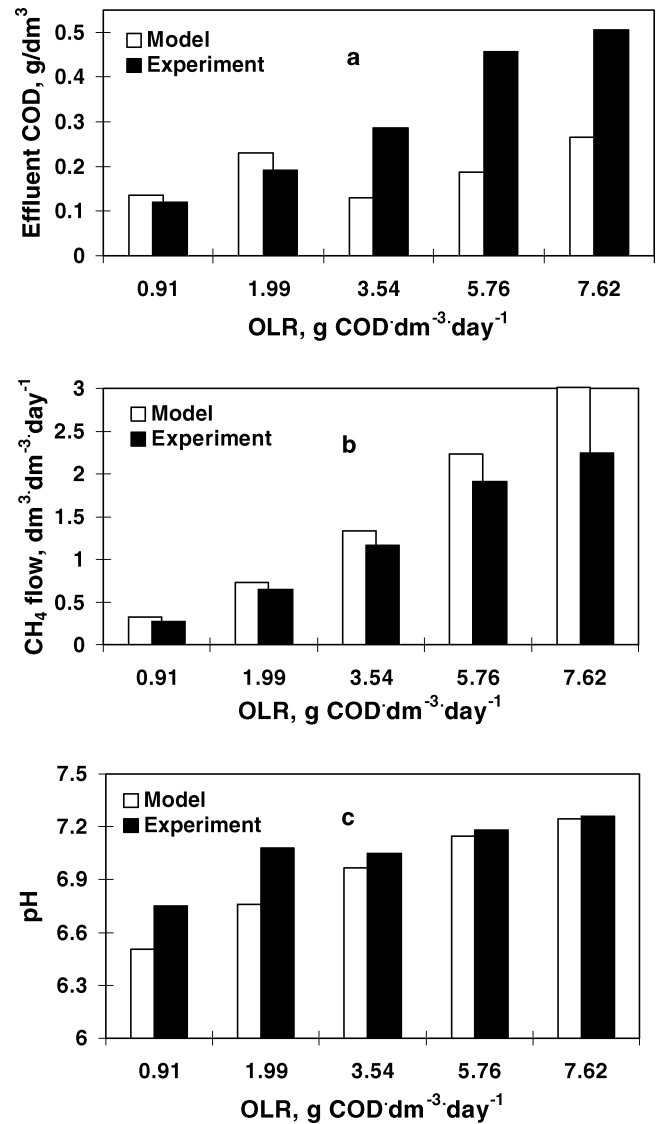


Fig. 3a–c Performance of the UASB reactor operating under steady-state conditions: model vs experimental data of Yan et al. [37]. **a** Effluent COD, **b** methane production, **c** pH

ing, and their initial concentrations are quickly altered after start-up. The sensitivity of the model to the average aggregate diameter of the seed sludge, especially towards aggravation, is as expected (Fig. 7b) because it has a direct influence on sludge settleability during the start-up period and, consequently, on the treatment efficiency of a UASB reactor.

The results of the sensitivity analysis for bacterial parameters are summarised in Fig. 8. In general, the growth parameters of bacterial groups X_2 and X_4 (especially μ_m) are the factors to which the model is most sensitive (Fig. 8a–c). Hence, determination of these parameters is of utmost importance for the application of this model in practice. The sensitivity of the model to the growth parameters of the remaining bacterial groups is moderate-to-small, conform the sensitivity results discussed in the previous paragraph.

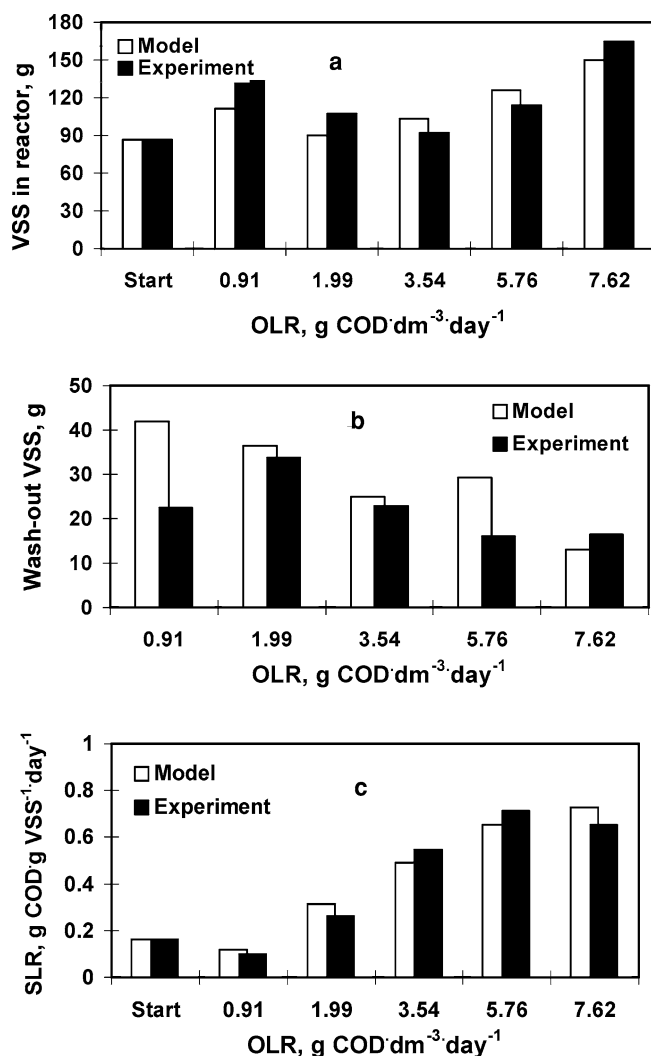


Fig. 4a–c Sludge characteristics at the end of each OLR applied. Model vs experimental data of Yan et al. [37]. a Total VSS in reactor at the end of each period, b integral VSS wash-out during each period, c SLR at the end of each period

The very low sensitivity of the model to the decay/lysis coefficients (data not shown) is a priori predictable due to the relative slowness of decay processes in comparison with sludge growth and wash-out under mesophilic conditions [29]. The enormous sensitivity of the model to the lower drop-off value pK (50% inhibition of growth rate) of acetotrophic methanogens (Fig. 8d) is also not surprising taking into account the primary role of these bacteria in resistance of the reactor against acidification.

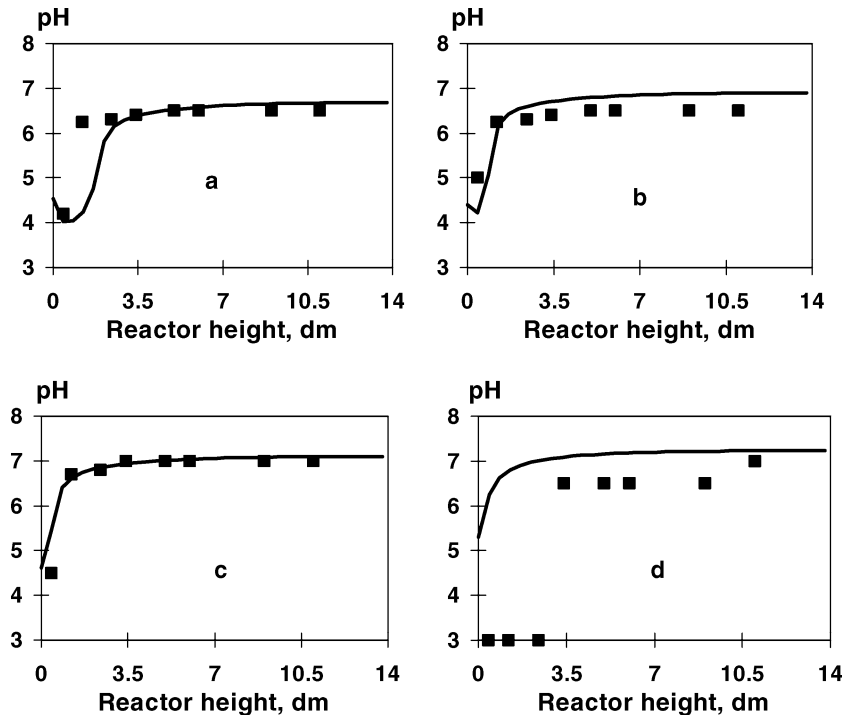
Since both the ψ -parameters directly influence the reactor solids dynamics, the corresponding sensitivity analysis is better illustrated by the dynamics of total VSS in the reactor (Fig. 9). The 20% decrease in both parameters [ψ_1 $\rho_{ag-\rho L}$] (Fig. 9a) and ψ_2 (Fig. 9b) from the basic values listed in Table 4 leads to a gradual wash-out of the sludge from the reactor. As a result, the reactor fails already during period II due to acidification (data not shown).

Model application

The model developed allows additional information about the UASB reactor under investigation to be derived. As a first example, Fig. 10 presents the calculated concentration profiles of total VSS and acetotrophic methanogens (the most important bacteria in the system) along the reactor height at the end of each experimental period. Figure 10a clearly shows that the height of the high-density sludge zone (sludge bed) varies significantly under the various operational regimes applied. Namely, this height significantly decreased during the first two periods of operation due to increased sludge wash out during this period (Fig. 4b). However, continuous improvement of the settling characteristics of the remaining sludge (Fig. 1b) during periods III–V led to a gradual increase in the sludge bed height followed by a substantial elevation of VSS concentration in this zone (Fig. 10a). Interestingly, at a low OLR of 1.91 g COD dm⁻³ day⁻¹, there is a sharp distinction between the sludge bed (high and constant solid concentration) and the sludge blanket (lower and gradually decreasing solid concentration). This sharp distinction disappears during subsequent increases in OLR (Fig. 10a). Thus, due to the continuous description of sludge dynamics along the reactor height, the dispersed plug-flow model is able to predict the position as well as the granular sludge concentration gradient at the boundary between the sludge bed and sludge blanket zones in a UASB reactor. To the best of our knowledge, no previously reported model of UASB reactors possesses this ability without any arbitrary division of the reactor volume into different zones with postulated mixing regimes. It should also be noted that subsequent increases in OLR led to a significant enrichment of the sludge by acetotrophic methanogens (Fig. 10b), which agrees with many other experimental observations [1, 12, 31]. However, the model also predicts that even a sludge with a substantial enrichment of acetotrophic methanogens (e.g. at the end of period V) cannot cope with a heavy overloading of the reactor, as indicated by a simulation where the OLR was doubled in comparison with the OLR applied during period V (data not shown). In the latter case, the reactor failed because VFA production exceeded the assimilative methanogenic capacity of the sludge.

As a second example of the potential of the dispersed plug flow model to obtain insight into UASB operation, Fig. 11 presents the influence of the height/diameter ratio of a UASB reactor on its performance. A decrease in this ratio in comparison with the applied experimental configuration (height/diameter ratio of 12; Table 1) is seen to lead to better reactor performance, especially during the first two periods (Fig. 11a) when the settling characteristics of the sludge were poor. Better reactor performance under lower reactor height/diameter ratio can be explained by the lower surface gas production rate (Eq. 20), resulting in lower values

Fig. 5 Model vs experiment for the pH profiles along the reactor height after an operating period of three HRTs at an OLR (g COD dm⁻³ day⁻¹) of **a** 1.99, **b** 3.54, **c** 5.76, **d** 7.82. Data points Experimental data of Yan et al. [37], lines model



of the dispersion coefficient (Eq. 12), consequently leading to less sludge wash-out (Fig. 11b). In contrast, a higher reactor height/diameter ratio leads to increased sludge washout during the first period of operation (Fig. 11b), thus yielding a slightly poorer treatment efficiency (Fig. 11a). However, after the initial elevated sludge washout in the taller reactor, this trend decreased through periods II–V (Fig. 11b) because of the good settling characteristics of the sludge remaining in the reactor. Thus, start-up of tall reactors requires primary attention to the settling characteristics of the seed sludge to prevent excessive washout. This recommendation conforms to existing practice relating to tall reactor start-up [e.g. internal circulation (IC) reactors up to 20 m high] with only granular sludge with excellent settling characteristics. For less tall reactors (UASB reactors of 2–3 m), the settling characteristics of the seed sludge are less important because the gas-induced dispersion of the solids is not as intensive in these reactor configurations.

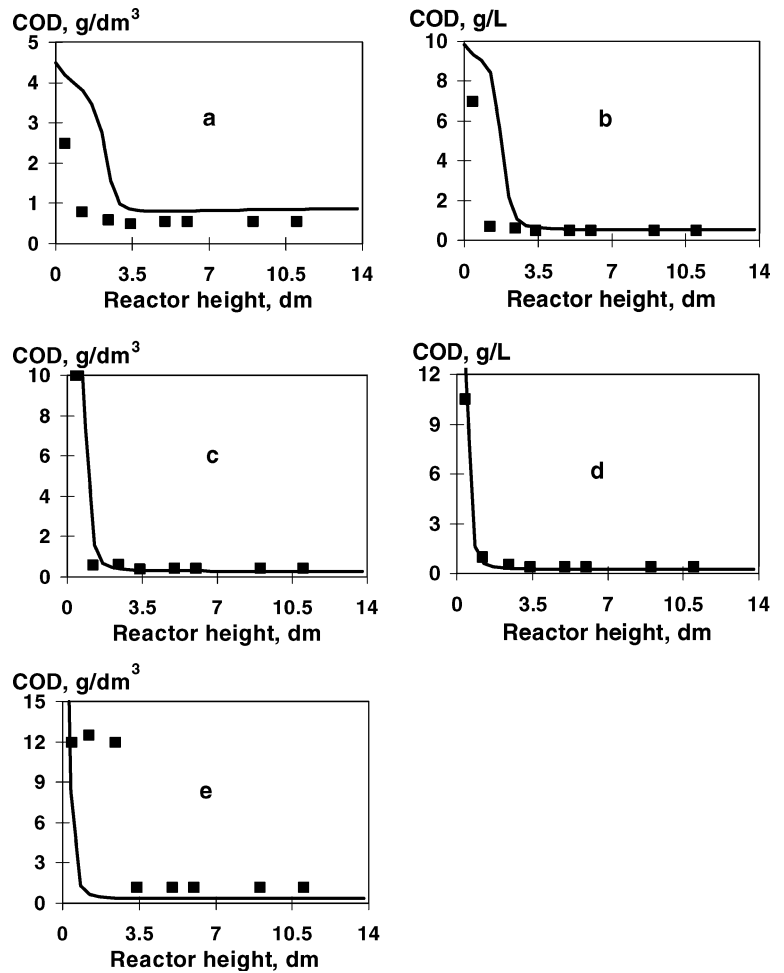
Interestingly, a small and broad reactor configuration demonstrates a very narrow acidified zone at the bottom of the reactor, especially under low OLR (Fig. 11c), in comparison with the taller reactors. This is due to the extremely low values of the dispersion coefficients (23–29 dm² day⁻¹) generated in the reactor bottom, resulting in an almost plug-flow regime in that section. However, this difference disappears almost completely when applying a high OLR (Fig. 11d) due to good mixing conditions throughout the reactor volume in all the configurations considered. In the latter case, large values of dispersion coefficients (>2,000 dm² day⁻¹) are generated, even at the reactor bottom due to the high surface gas production rates.

Conclusions

This paper presents a newly developed dispersed plug flow model of UASB reactors (Eqs. 1, 2, 3, 4, 5, 6, 7, 8, 9, 10, 11, 12, 13, 14, 15, 17, 18, 19, 20, 21, 22, 23, 24, 25, 26, 27, 28, 29), based on the combination of sludge dynamics and bacterial metabolism. To our knowledge, this is the first successful attempt in the creation of models of a new generation that are able to simulate complex space heterogeneous dynamics, not only of solutes but also of the granular sludge (e.g. imminent formation and development of sludge bed and blanket zones, sludge wash-out) inside UASB reactors. The second principal difference of the presented model with previously proposed models of UASB reactors [3, 36] is that it provides a universal description of both hydrodynamics and solids dynamics by continuous equations throughout the reactor volume. The third prominent feature of the dispersed plug flow model is that it relies solely on internal mechanisms of the bioprocesses to predict sludge washout from the reactor. This feature is a distinct advantage over the approach used worldwide to model anaerobic reactors with a fixed sludge retention time. The latter was routinely transferred from activated sludge reactor models but can no longer be considered valid, at least for the description of high-rate anaerobic reactors, because of the principal differences between these treatment systems. The above-mentioned abilities of the described dispersed plug flow model make this type of mathematical model a powerful tool in the design and control of UASB reactors, as illustrated in Figs. 10 and 11.

Despite its conceptual advantages over models proposed thus far, the described model also used some

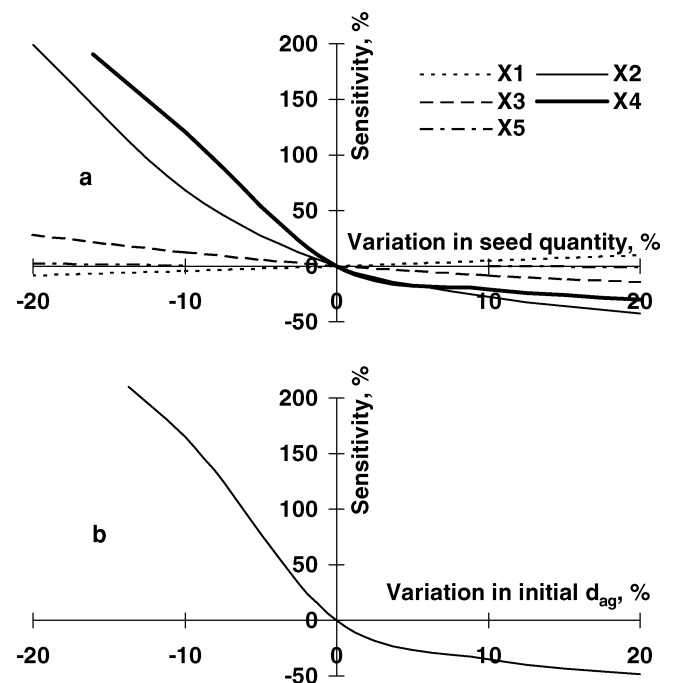
Fig. 6 Model vs experiment for the COD profiles along the reactor height after an operating period of three HRTs at an OLR (g COD dm⁻³ day⁻¹) of **a** 0.91, **b** 1.99, **c** 3.54, **d** 5.76, **e** 7.82. *Data points* Experimental data of Yan et al. [38], *lines* model



assumptions and empirical equations, which require further fine-tuning. It should, nevertheless, be noted that so far no alternative mathematical expressions are

available for the empirical relations adopted in the present paper to describe the time dependency of the average aggregate diameter and sludge density. Further

Fig. 7a,b Sensitivity of the dispersed plug flow model to changes in seed sludge characteristics. The relative variation of the effluent COD at day 15 (period of three HRTs) was defined as the sensitivity: variation in **a** initial quantity of various bacteria X_j involved in the seed and **b** initial aggregate diameter



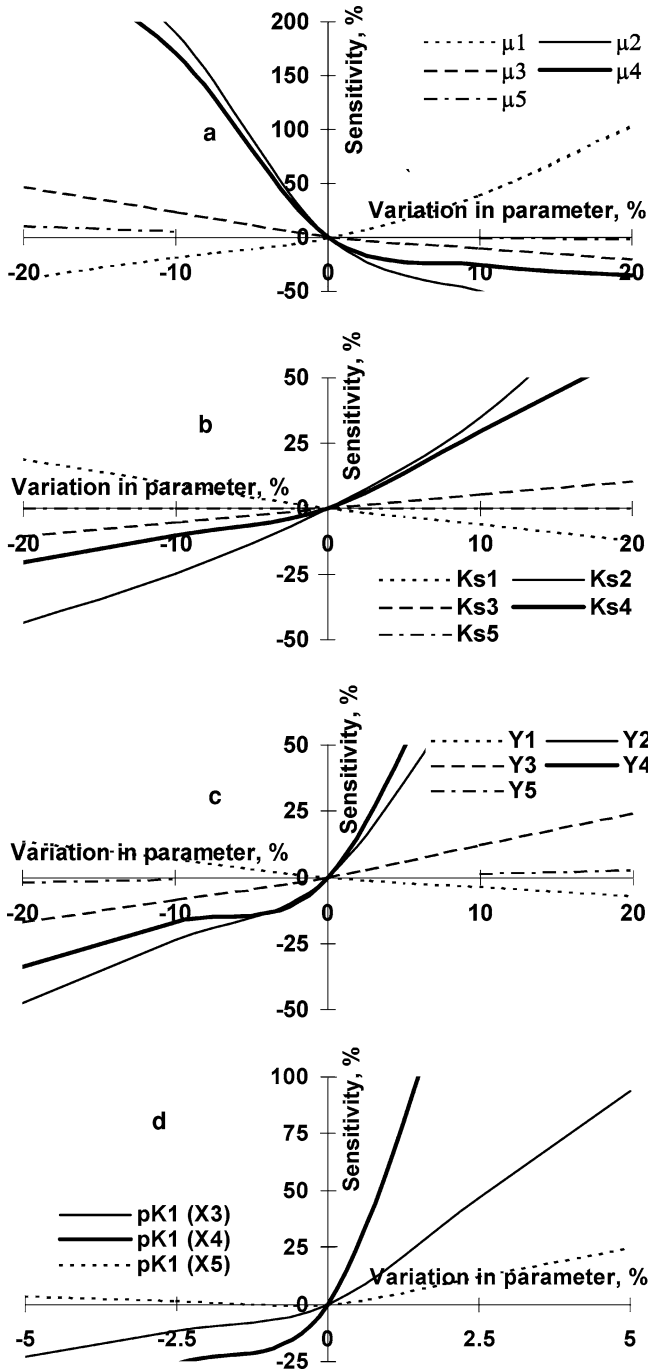


Fig. 8a–d Sensitivity of the dispersed plug flow model to changes in the bacterial parameters. The relative variation of the effluent COD at day 15 was defined as the sensitivity: variation in **a** $\mu_{m,j}$, **b** $K_{s,j}$, **c** Y_j , **d** pK_1 for acetogens and methanogens

research to derive these relations is required to fine-tune the developed mathematical model. The parameter sensitivity analysis showed that the growth properties of protein-degrading bacteria and acetotrophic methanogens (especially μ_m) as well as the sludge settleability characteristics ψ_1 and ψ_2 are the parameters that influence a UASB reactor most. The kinetic properties of the bacteria involved in anaerobic digestion have received extensive attention in the literature (see, e.g. [29]). In

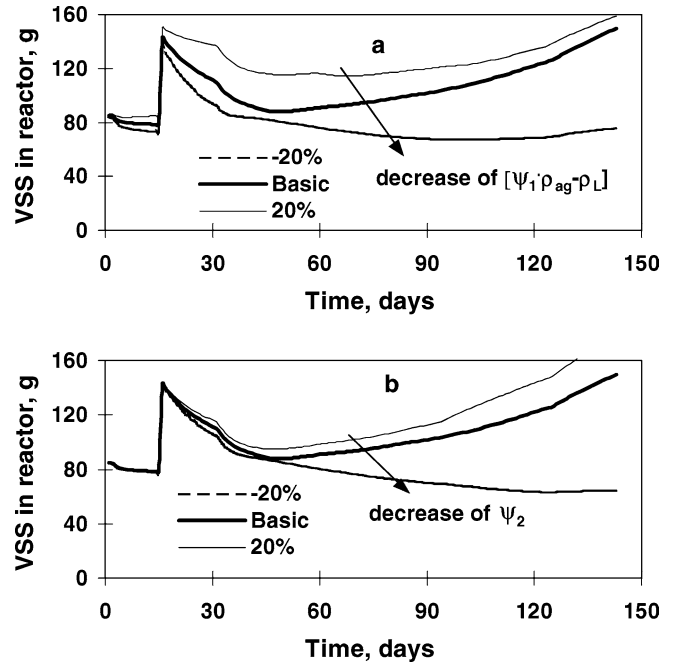


Fig. 9a,b Sensitivity analysis of the sludge settleability parameters. Effect of a 20% increase and decrease in **a** $[\psi_1 \rho_{ag} - \rho_L]$, and **b** ψ_2 on the modelling results of the total VSS present in the reactor

contrast, internal sludge dynamics in UASB reactors have rarely been studied, which hampers further comprehensive validation, justification and development of the dispersed plug flow model. Therefore, further elucidation of the internal mechanisms of the functioning of UASB reactors, which will allow the present model to be upgraded, will require new comprehensive experimental studies including both traditionally measured “black box” characteristics (overall reactor performance, gas production, etc.), supplemented with detailed documentation of the profiles of COD, VFA, VSS, specific metabolic activity, aggregate diameter, and density along the reactor height.

Acknowledgements We thank Dr. Robbert Kleerebezem for critical suggestions on the manuscript and Prof. G. Lettinga for stimulating discussions during the preparation of the manuscript. This work was part of a research project supported by The Netherlands Organization for Scientific Research (Grant N299825).

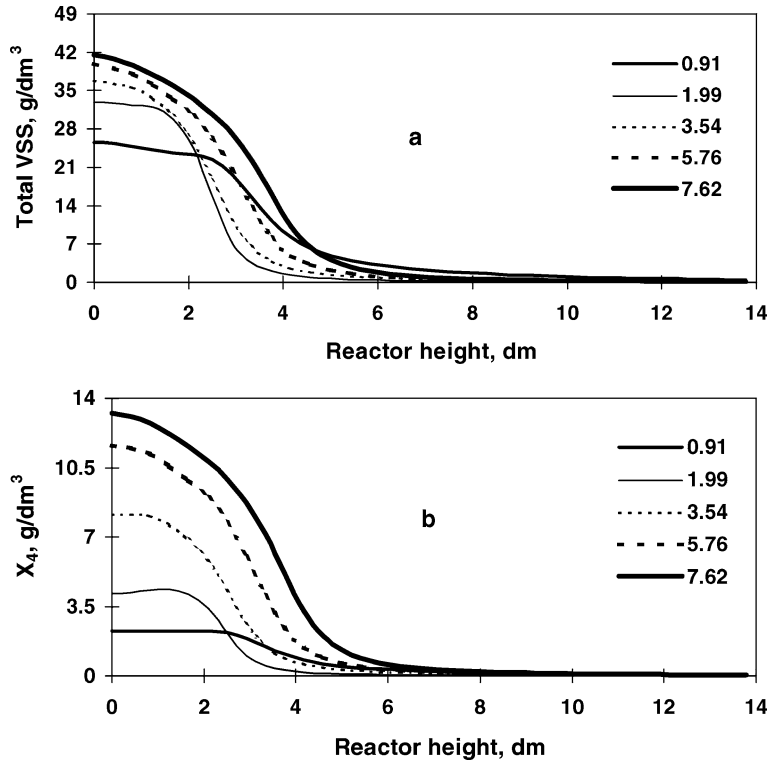
Appendix 1: General form of material balances for the components involved

Gas phase

The partial pressure p_i of a gaseous substrate i in the gas volume is calculated by a component balance around the gas phase:

$$\frac{dp_i(t)}{dt} = \frac{p_{tot} \cdot V_{m,i} \cdot \left(\int_0^H M_i(z,t) \cdot CS \cdot dz \right) - p_i \cdot Q_{tot}(t)}{V_G} \quad (17)$$

Fig. 10 Model simulations of the concentration profiles of **a** total VSS and **b** acetotrophic methanogens, X_4 , along the reactor height at the end of each OLR applied (figures on the plots refer to the applied OLR, expressed in $\text{g COD dm}^{-3} \text{ day}^{-1}$)



where:

$M_i(z)$ = mass transfer rate of substrate i to the gas phase from the compartment z :

$$M_i(z, t) = k_L a(z, t) \cdot \left(S_i^*(z, t) - \frac{p_i(t)}{H_{e_i}} \right) \quad (18)$$

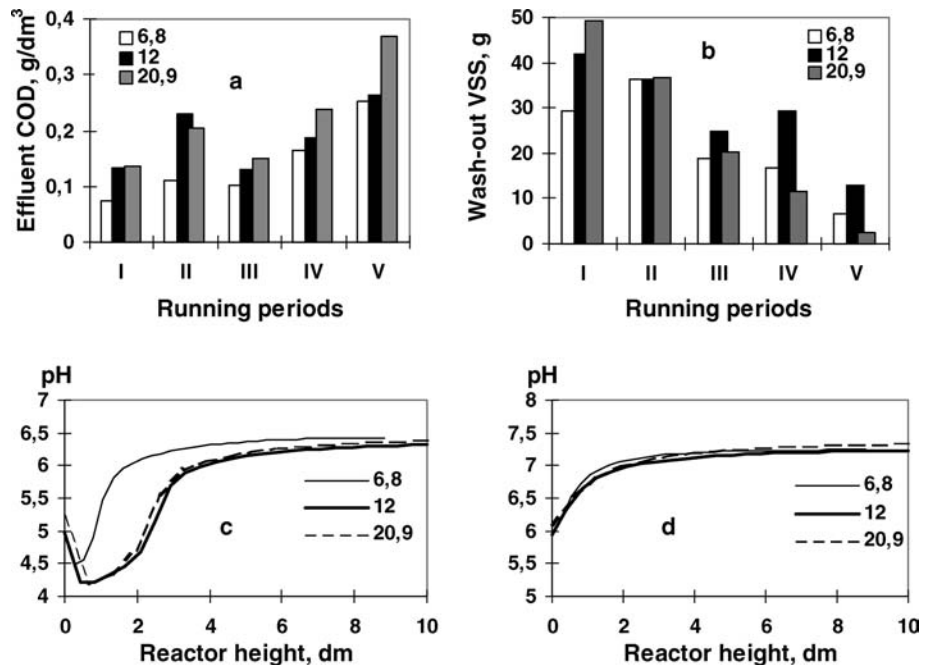
p_{tot} = total pressure in the reactor head space ($p_{\text{tot}} = \sum p_i$, p_{tot} was accepted to be equal to 1 atm).

A total balance gives the gas volumetric flow rate, Q , from the reactor:

$$Q_{\text{tot}}(t) = \sum_i V_{m,i} \int_0^H M_i(z, t) \cdot CS \, dz \quad (19)$$

A gas flow passing through a fixed cross-section CS_z equals:

Fig. 11 Model simulations showing the impact of the reactor height/diameter ratio (figures on the plots) on **a** effluent COD, **b** VSS wash-out for the experimental period, and **c, d** the pH profiles along the reactor height after an operating period of three HRTs at an OLR of 0.91 (**c**) and 7.82 (**d**) $\text{g COD dm}^{-3} \text{ day}^{-1}$. A reactor height/diameter ratio of 12 corresponds to the size of the UASB reactor used in the experimental study of Yan et al. [38]. Variation in the height/diameter ratio maintained a constant working volume of the reactor



$$q(z, t) = \sum_i V_{m,i} \int_0^z M_i(z, t) \cdot dz \quad (20)$$

Liquid phase

A general material balance for soluble substrates can be written on the basis of Eq. 1 as:

$$\begin{aligned} \frac{\partial}{\partial t} S_i(z, t) = & \frac{\partial}{\partial z} \left[D(z, t) \cdot \frac{\partial}{\partial z} S_i(z, t) \right] - W_{up} \cdot \frac{\partial}{\partial z} [S_i(z, t)] \\ & + \sum_j [\mu_j(z, t) \cdot X_j(z, t) / Y_j + b_j \cdot X_j(z, t) \\ & \cdot (1 - \theta \cdot Y_j)] - M_i(z, t) \end{aligned} \quad (21)$$

M_i for non-gaseous substrates are equal to zero. D_i are accepted to be the same for all substrates and determined by Eq. 12. The corresponding boundary conditions are the following:

$$z = 0 \quad W_{up} \cdot S_i^0(t) = W_{up} \cdot S_i(0, t) - D(0, t) \cdot \frac{dS_i(0, t)}{dz} \quad (22)$$

$$z = H \quad \frac{dS_i(H, t)}{dz} = 0 \quad (23)$$

A general mass balance equation used to describe the behaviour of each bacterial group j in the reactor is presented in Eq. 24:

$$\begin{aligned} \frac{\partial}{\partial t} X_j(z, t) = & \frac{\partial}{\partial z} \left[D(z, t) \cdot \frac{\partial}{\partial z} X_j(z, t) \right] \\ & - \frac{\partial}{\partial z} [W(z, t) \cdot X_j(z, t)] + (\mu_j(z, t) - b_j) \\ & \cdot X_j(z, t) \end{aligned} \quad (24)$$

For simplicity, D_j and W_j are accepted to be the same for all bacterial groups. W_j (for $z < H$) and D_j were calculated from Eqs. 4 and 12, respectively. To take into account wash-out of biomass, W_j in the last compartment was accepted to be equal to W_{up} . Thus, the boundary conditions can be presented as follows:

$$z = 0 \quad W(0) \cdot X_i(0, t) = D(0, t) \cdot \frac{dX_i(0, t)}{dz} \quad (25)$$

$$z = H \quad W(H) \cdot X_i(H, t) = D(H, t) \cdot \frac{dX_i(H, t)}{dz} \quad (26)$$

Since not all reactor VSS represents active biomass [33], an additional equation for biologically inactive VSS introduced with the seed sludge was incorporated in the model. The corresponding mass balance equation and boundary conditions are:

$$\begin{aligned} \frac{\partial}{\partial t} \text{VSS}_{\text{inact.}}(z, t) = & \frac{\partial}{\partial z} \left[D(z, t) \cdot \frac{\partial}{\partial z} \text{VSS}_{\text{inact.}}(z, t) \right] \\ & - \frac{\partial}{\partial z} [W(z, t) \cdot \text{VSS}_{\text{inact.}}(z, t)] \\ & - b_{\text{inact.}} \cdot \text{VSS}_{\text{inact.}}(z, t) \end{aligned} \quad (27)$$

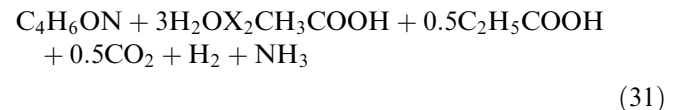
$$z = 0 \quad W(0) \cdot \text{VSS}_{\text{inact.}}(0, t) = D(0, t) \cdot \frac{d\text{VSS}_{\text{inact.}}(0, t)}{dz} \quad (28)$$

$$z = H \quad W(H, t) \cdot \text{VSS}_{\text{inact.}}(H, t) = D(H, t) \cdot \frac{d\text{VSS}_{\text{inact.}}(H, t)}{dz} \quad (29)$$

The current version of the model neglects the contribution of bacterial decay to the amount of biologically inert VSS in the system. This assumption is justified by the fact that the sensitivity of the model to the parameters b_j is very low (see above).

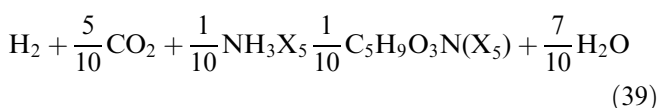
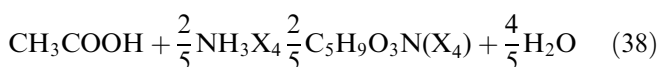
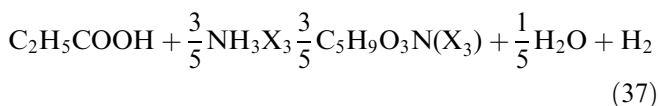
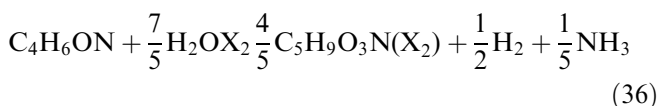
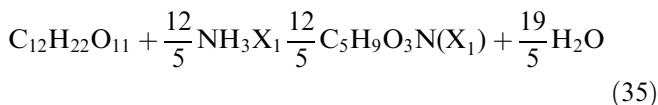
Appendix 2 Model specification for the case of cheese whey treatment

It is known that cheese whey consists mainly of proteins, lactose and VFA [22], and thus these components were chosen as influent substrates in our model. Using the average protein formula C_4H_6ON [29] and the median values of COD, TKN, NH_4^+ -N, NO_3^- -N and VFA from Table 1, the total influent COD can be decomposed into its constituents as lactose:protein:VFA = 0.5:0.46:0.04 (on a COD basis). Since only acetate and propionate were detected as intermediates in the experiments of Yan et al. [37, 38], the simplified reaction sequence by which the cheese whey constituents are transformed by the different groups of anaerobic bacteria in a UASB reactor are presented below:

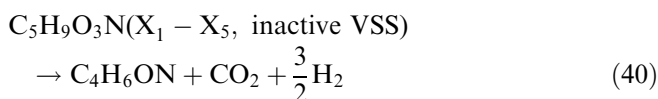


The following five trophic groups of microorganisms are involved: group X_1 contains all saccharolytic bacteria;

X₂, all proteolytic bacteria; X₃, all propionate-degrading bacteria; X₄, all acetotrophic methanogens and X₅, all hydrogenotrophic methanogens. The stoichiometry of their growth is given below (cell mass and inactive VSS is represented by empirical formula C₅H₉O₃N [25]):



To keep an accurate material balance in the system, bacterial lysis as source of biodegradable organic matter should be taken into account. This is especially important for UASB reactors, which usually have very long sludge retention times, up to more than 100 days. In the model, this was done by the introduction of Eq. 40, i.e. bacterial lysis resulted in the formation of soluble "protein" as the main product. The same reaction was used for decomposition of inactive VSS:



References

- Alphenaar A (1994) Anaerobic granular sludge: characterization, and factors affecting its functioning. PhD thesis, Wageningen Agricultural University, The Netherlands
- Bailey JE, Ollis DF (1986) Biochemical engineering fundamentals, 2nd edn. McGraw-Hill, New York
- Bolle WL, van Breugel J, van Eybergen GC, Kossen NWF, Zoetemeyer RJ (1986) Modeling the liquid flow in p-flow anaerobic sludge blanket reactor. *Biotechnol Bioeng* 28:1615–1620
- Buffiere P, Fonade C, Moletta R (1998) Mixing and phase hold-ups variations due to gas production in anaerobic fluidized-bed digesters: influence on reactor performance. *Biotechnol Bioeng* 60:36–43
- Chang HT, Rittman BE (1987) Mathematical modeling of biofilm on activated carbon. *Environ Sci Technol* 21:273–280
- Cohen A, Breure AM, van Andel JG, van Deursen A (1982) Influence of phase separation on the anaerobic digestion of glucose. II. Stability and kinetic responses to shock loading. *Water Res* 16:449–457
- Darton RC (1985) The physical behaviour of three-phase fluidized beds. In: Davidson JF, Clift R, Harrison D (eds) *Fluidization*, 2nd edn. Academic, London, pp 495–525
- Davison BH (1989) Dispersion and holdup in a three-phase fluidized bed bioreactor. *Appl Biochem Biotechnol* 20/21:449–460
- Grotenhuis JTC, Kissel JC, Plugge CM, Stams AJM, Zehnder AJM (1991) Role of substrate concentration in particle size distribution of methanogenic granular sludge in UASB reactor. *Water Res* 25:21–27
- Heertjes PM, Kuijvenhoven LJ (1982) Fluid flow pattern in upflow reactors for anaerobic treatment of beet sugar factory wastewater. *Biotechnol Bioeng* 24:443–459
- Heertjes PM, van der Meer RR (1978) Dynamic of liquid flow in an upflow reactor used for anaerobic treatment of wastewater. *Biotechnol Bioeng* 20:1577–1594
- Hulshoff Pol LW (1989) The phenomenon of granulation of anaerobic sludge. PhD thesis, Wageningen Agricultural University, The Netherlands
- Kafarov VV, Dorokhov IN (1976) System analysis of processes of chemical technology: bases of strategy (in Russian). Nauka, Moscow
- Kalyuzhnyi SV (1997) Batch anaerobic digestion of glucose and its mathematical modelling. II. Description, verification and application of model. *Bioresour Technol* 59:249–258
- Kalyuzhnyi S, Fedorovich V (1997) Integrated mathematical model of UASB reactor for competition between sulphate reduction and methanogenesis. *Water Sci Technol* 36:201–208
- Kalyuzhnyi SV, Fedorovich VV (1998) Mathematical modelling of competition between sulphate reduction and methanogenesis in anaerobic reactors. *Bioresour Technol* 65:227–242
- Kalyuzhnyi S, Fedorovich V, Lens P, Hulshoff Pol L, Lettinga G (1998) Mathematical modelling as a tool to study population dynamics between sulfate reducing and methanogenic bacteria. *Biodegradation* 9:187–199
- Korn GA, Korn TM (1968) *Mathematical handbook for scientists and engineers*. McGraw-Hill, New York
- Lettinga G (1996) Sustainable integrated biological wastewater treatment. *Water Sci Technol* 33:85–98
- Lettinga G, van Velsen AFM, Hobma SW, de Zeeuw WJ, Klapwijk A (1980) Use of the upflow sludge blanket (USB) reactor concept for biological wastewater treatment, especially for anaerobic treatment. *Biotechnol Bioeng* 22:699–734
- Levenspiel O (1972) *Chemical reaction engineering*, 2nd edn. Wiley, New York
- Mawson AJ (1994) Bioconversion for whey utilization and waste abatement. *Bioresour Technol* 47:195–203
- Millne WI (1955) *Numerical solution of differential equations*. Inostrannaya literatura, Moscow
- Morvai L, Mihaltz P, Czako L, Hollo J (1990) The influence of organic load on granular sludge development in an acetate fed system. *Appl Microbiol Biotechnol* 33:463–468
- Mosey FE (1983) Mathematical modeling of anaerobic digestion process: regulatory mechanisms for the formation of short-chain volatile acids from glucose. *Water Sci Technol* 15:209–217
- Narnoli SK, Mehrotra I (1997) Sludge blanket of UASB reactor: mathematical simulation. *Water Res* 31:715–726
- Omil F, Lens P, Hulshoff Pol L, Lettinga G (1997) Characterization of biomass from a sulphidogenic, volatile fatty acid-degrading granular sludge reactor. *Enzyme Microb Technol* 20:229–236
- Parulekar SJ, Shash YT (1980) Steady-state behavior of gas-liquid-solid fluidized-bed reactors. *Chem Eng J* 20:21–33
- Pavlostathis SG, Giraldo-Gomez E (1991) Kinetics of anaerobic treatment: a critical review. *Crit Rev Environ Control* 21:411–490
- Rabinovich VL, Havin ZYa (1977) *Short chemical handbook*. Khimiya, Moscow
- Rebac S (1998) Psychrophilic anaerobic treatment of low strength wastewaters. PhD thesis, Wageningen Agricultural University, The Netherlands

32. Samarskiy AA (1987) Introduction into numerical methods. Nauka, Moscow
33. Schmidt JE, Ahring BK (1996) Granular sludge formation in upflow anaerobic sludge blanket reactors. *Biotechnol Bioeng* 49:229–246
34. Smith DN, Ruether JA (1985) Dispersed solid dynamics in a slurry bubble column. *Chem Eng Sci* 40:741–754
35. Webb OF, Davison BH, Scott TC (1996) Modeling scale-up effects on a small pilot scale fluidized bed reactor for fuel ethanol production. *Appl Biochem Biotechnol* 57/58:639–647
36. Wu MM, Hickey RF (1997) Dynamic model for UASB reactor including reactor hydraulics, reaction and diffusion. *J Environ Eng ASCE* 123:244–252
37. Yan JQ, Lo KV, Liao PH (1989) Anaerobic digestion of cheese whey using up-flow anaerobic sludge blanket reactor. *Biol Wastes* 27:289–305
38. Yan JQ, Lo KV, Pinder KL (1993) Instability caused by high strength of cheese whey in a UASB reactor. *Biotechnol Bioeng* 41:700–706
39. Zhukova TB (1991) Investigation and modeling of bubble column reactors (in Russian). *Itogi Nauki i Tekhniki, Ser. Processes and apparatuses of chemical technology*, vol 18. VINITI Press, Moscow
40. Zoetemeyer RJ (1982) Acidogenesis of soluble carbohydrate containing waste waters. PhD thesis, University of Amsterdam, The Netherlands